SPE 93296

Interpretation of Skin Effect from Pressure Transient Tests in Horizontal Wells

A.M. Al-Otaibi, SPE, Technological College of Studies, E. Ozkan, SPE, Colorado School of Mines

This paper was prepared for presentation at the 14th SPE Middle East Oil & Gas Show and Conference held in Bahrain International Exhibition Centre, Bahrain, 12–15 March 2005.

Abstract

Most horizontal wells have non-uniform distribution of skin along their lengths and this creates a challenging problem in the interpretation of their pressure-transient responses. The theory indicates that the rigorous incorporation of non-uniform skin distribution into horizontal well pressure-transient models requires the knowledge of not only the skin distribution but also the flow rate distribution into the horizontal well from the reservoir. Because this information is not normally available to the analyst, standard pressure interpretation techniques and tools assume uniform distribution of skin with the expectation that the estimates would correspond to some average of the skin distribution. The question that has not been adequately addressed in the literature is the physical meaning of the skin estimates from different pressure-transient analysis tools in common use. Because this question has not been adequately addressed, purely geometrical interpretations of the skin estimates have been proposed to calculate horizontal well productivities and develop flow models.

In this paper, we generate synthetic pressure-transient responses for different non-uniform skin distributions along a horizontal well and analyze these responses by using the conventional tools that assume uniform distribution of skin. Skin estimates from well-test interpretation are then compared with the known skin distributions.

The findings of this study are practical and important. First, the pressure drop caused by skin depends on the flow regimes if the skin distribution is non-uniform. Because the models used in commercial software assume the same additional pressure drop due to skin, the regression analysis can only match one of the flow periods for a constant skin value. To interpret the meaning of this skin estimate, we used the semi-log analysis techniques and demonstrated what type of average the estimated skin represents for different flow regimes and different skin distributions. For most cases, the estimates of skin from early-time radial flow analysis represent the arithmetic average of the skin distribution which may be useful for stimulation decisions. The skin estimate from the pseudo-radial flow period corresponds to the skin pressure drop at the heel of the horizontal well, which represents the additional pressure drop to be considered in the productivity calculations. We demonstrate that the geometric interpretation of the non-uniform skin effect proposed in the literature is inaccurate and leads to significant errors in the calculation of horizontal well productivity.

Horizontal Well Skin Factor

Van Everdingen[1] and Hurst[2] defined the concept of skin for vertical wells which quantifies the severity of the formation damage. The relation between the skin factor and the permeability and radius of the damaged zone is given by Hawkins' relation.[3] In the literature, many researchers have demonstrated that formation damage varies from the heel to the toe in especially long horizontal wells[4-14]. In this section, we present the derivations of horizontal well skin factor following Ozkan and Raghavan.[15,16]

The horizontal well model shown in Fig. 1 was used in the derivations of the horizontal well skin factor. The horizontal well is located at an elevation, z_w, with respect to the bottom boundary and has a length, L_h, along the x-axis. The radial distance in the vertical, y-z plane is defined as $\tilde{r}$. The skin zone is assumed to be concentric with the horizontal well and has a radius, $\tilde{r}_s$, that is a function of the location along the horizontal well. The effective permeability in the y-z plane is defined as k_r while the effective permeability of the skin zone is defined as k_s. The flow within the skin region as defined above is assumed to be normal to the well axis (i.e. in the r-direction). This is because the radius of the skin zone is small (thin skin). If the storage capacity of the skin zone is negligibly small as implied by the thin skin assumption, then the fluxes entering and leaving the skin zone are identical (that is $q_h(\tilde{r}_s,x,t) = q_h(\tilde{r}_w,x,t) = q_h(x,t)$). Since the flux is a function of the properties of the skin zone, q_h represent the flux when there is no skin and q_{hs} represents the flux when there is skin.

The flux passing through the skin zone (ring of radius $\tilde{r}_s$ centered at y = 0 or z = z_w) is given by

$$q_h(x,t) = 7.08x10^{-3}\frac{k_{\tilde{r}}}{\mu}\left(\tilde{r}\frac{\partial p}{\partial \tilde{r}}\right) \qquad (1)$$

Integrating Eq. 1 to obtain the pressure drop across the skin zone, we obtain

$$p_s(\tilde{r}_s,x,t)-p_s(\tilde{r}_w,x,t)=\frac{141.2\mu}{k_s}q_{hs}(x,t)\ln(\frac{\tilde{r}_s}{\tilde{r}_w}) \quad (2)$$

If there is no damage, the permeability in the skin zone is the same as the permeability in the reservoir. Then, the pressure drop across the skin zone is given by

$$p(\tilde{r}_s,x,t)-p(\tilde{r}_w,x,t)=\frac{141.2\mu}{k_{\tilde{r}}}q_h(x,t)\ln(\frac{\tilde{r}_s}{\tilde{r}_w}) \quad (3)$$

Let us define the additional pressure drop due to skin by

$$\Delta p_s(x,t)=p_{wf,ideal}-p_{wf,actual} \quad (4)$$

The additional pressure drop due to skin is the difference between the wellbore pressure for the no-skin case and the wellbore pressure for the damaged well; that is,

$$p_{wf,ideal}=p(\tilde{r}_w,x,t) \quad \text{and} \quad p_{wf,actual}=p_s(\tilde{r}_w,x,t).$$

Then, from Eqs. 2, 3, and 4, we obtain

$$\Delta p_s(x,t)=\frac{141.2q_{hs}\mu}{k_{\tilde{r}}}\left(\frac{k_{\tilde{r}}}{k_s}-\frac{q_h}{q_{hs}}\right)\ln\frac{\tilde{r}_s}{\tilde{r}_w}+\left[p(\tilde{r}_s,x,t)-p_s(\tilde{r}_s,x,t)\right] \quad (5)$$

If we assume that the difference between the pressures at the skin boundary with and without skin is negligible, then Eq. 5 becomes

$$\Delta p_s(x,t)=\frac{141.2q_{hs}\mu}{k_{\tilde{r}}}\left(\frac{k_{\tilde{r}}}{k_s}-\frac{q_h}{q_{hs}}\right)\ln\frac{\tilde{r}_s}{\tilde{r}_w} \quad (6)$$

A dimensionless mechanical skin factor, S_{hm}, can be defined from Eq. 6 as follows:

$$S_{hm}(x,t)=\frac{\frac{kh}{141.2q\beta\mu}\Delta p_s(x,t)}{q_{hD}(x_D,t_D)}=\frac{k}{k_{\tilde{r}}}\frac{h}{L}\left[\frac{k_{\tilde{r}}}{k_s}-\frac{q_h(x,t)}{q_{hs}(x,t)}\right]\ln\frac{\tilde{r}_s}{\tilde{r}_w} \quad (7)$$

where

$$q_{hD}(x_D,t_D)=\frac{q_{hs}(x,t)L}{q\beta} \quad (8)$$

We should note the following observations from Eq. 7. Although we have followed the conventional derivation of skin factor, S_{hm} defined by Eq. 7 has some unconventional features. First, we assumed steady-state flow in the skin zone. This should indicate that $\Delta p_s/q_{hs}$ should be independent of time. Then, from the first equality in Eq. 7, the mechanical skin factor, S_{hm}, should be constant in time. This is consistent with the conventional understanding of skin factor. The second equality of Eq.7, however, indicates that unless q_h/q_{hs} is constant in time, S_{hm}, is time dependent. Later in this work we show that q_h/q_{hs} is time dependent; so there is an inconsistency between the first and second equalities of Eq. 7. The only case where q_h/q_{hs} is constant is when the flux distribution is uniform; that is when $q_h/q_{hs}=1$. In this case, the second equality of Eq. 7 reduces to the conventional thick skin formula of Muskat[17] and Hawkins'[3].

This discussion indicates that the conventional definition of skin for vertical wells (where the flux is uniform along a fully penetrating well) is not directly applicable to horizontal wells. Therefore, an alternative definition of mechanical skin and skin effect will be used as explained below.

Let us define the skin-zone pressure drop by

$$\Delta p_s(x,t)=p(\tilde{r}_s+,x,t)-p(\tilde{r}_w,x,t) \quad (9)$$

where $p(\tilde{r}_s+,x,t)$ represents the pressure immediately on the reservoir side of the skin boundary and $p(\tilde{r}_w,x,t)$ is the pressure recorded in the wellbore. We can define the mechanical skin factor by

$$S_{hm}(x)=\frac{\frac{kh}{141.2q\beta\mu}\Delta p_s(x,t)}{q_{hD}(x_D,t_D)} \quad (10)$$

Equation 10 is similar to Eq. 7 but Δp_s in Eq. 10 is defined by Eq. 9 instead of Eq. 4. Using Eq. 10, we can write

$$\frac{kh}{141.2q\beta\mu}\Delta p_s(x,t)=p_{wD}(\tilde{r}_{wD},x_D,t_D)-p_D(\tilde{r}_{sD}+,x_D,t_D)=q_{hD}(x_D,t_D)S_{hm}(x_D) \quad (11)$$

where p_{wD} and p_D are defined by

$$p_D=\frac{kh(p_i-p)}{141.2q\beta\mu} \quad (12)$$

Although Eq. 11 does not explicitly relate Δp_s to the actual properties of the skin zone as in Eq. 7, it is consistent in itself. If we also adopt the thin skin concept of Van Everdingen and Hurst[1,2], we obtain the following expression from Eq. 11:

$$p_{wD}(\tilde{r}_{wD},x_D,t_D)=p_D(\tilde{r}_{wD}+,x_D,t_D)+q_{hD}(x_D,t_D)S_{hm}(x_D) \quad (13)$$

where we used $p_D(\tilde{r}_{wD}+,x_D,t_D)=p_D(\tilde{r}_{sD}+,x_D,t_D)$ because the thin skin concept requires $\tilde{r}_{sD}+\rightarrow\tilde{r}_{wD}+$. Equation 13 will be used in this study to investigate the effect of skin factor.

Horizontal Well Pressure-Transient Model

The general pressure transient solution for horizontal wells is usually derived using the method of sources and sinks and green's functions[18]. Appendix A shows the derivations of the horizontal well pressure-transient model used in this study.

The next section presents a comparison of the results generated by our horizontal well model described in Appendix A with commercial well testing software (Saphir[20]).

Comparison with Commercial Software

The objective of the examples below is to compare the results of our model with those obtained by using commercial software.[20] Two cases were run with two different sets of data with and without skin. The data used in these cases are shown in Table 1.

Comparison Case 1.

First we check the uniform-flux solution by using only one segment in our model. Figure 2 shows the comparison of our results for Comparison Case 1 with the commercial software[20] for S_{hm} = 0 and 0.5. The agreement between the results is excellent.

Next we compare the pressure transient responses from this study with the commercial software for infinite-conductivity condition. To obtain the infinite-conductivity responses, we used 1, 20, and 40 segments in our model. Figure 3 indicates that after 20 segments, there is no discernable difference in the pressure responses and our solution matches with the results of the commercial software very well. (Usually more segments are required to obtain a good flux profile compared with pressure calculations). Figs. 4 and 5 show the corresponding flux distributions with 40 segments for S_{hm} = 0 and 0.5, respectively. As expected from the discussion above, flux profile is a function of time. In addition, skin effect tends to flatten the flux profile. Thus, the ratio of the fluxes with and without skin is not 1 except during the early times.

Comparison Case 2.

As shown in Fig. 6, the pressure generated for Comparison Case 2 by our model matched the pressure responses predicted by the commercial software[20] for two values of skin: S_{hm} = 0 and 0.75.

Estimation of Skin Effect from Horizontal-Well Pressure-Transient Tests

In this section, we will focus on the estimation of skin effect from horizontal-well pressure-transient tests. The semi-analytical horizontal well model introduced in Appendix A will be used in the discussions. We will demonstrate the importance of flux distribution on the estimation of skin factor.

For the discussions here, it is important to distinguish between a time independent skin factor and a time dependent skin effect. Physically, the skin factor can be used a measure of the formation damage while the skin effect is a measure of the skin pressure drop. The skin factor obtained from a well test is the skin effect, not the mechanical skin.

The mechanical skin factor, S_{hm}, is related to the skin effect, S, by the following equation (see Eq. 11):

$$S(x_D,t_D) = q_{hD}(x_D,t_D)S_{hm}(x_D) = \frac{kh}{141.2q\beta\mu}\Delta p_s \qquad (14)$$

Then, the time dependency of flux makes the skin effect time dependent also. For infinite-conductivity horizontal wells, the flux distribution is time dependent until it stabilizes at the onset of the late-time pseudo-radial flow. Also, the well-test-estimated skin effect corresponds to the heel of the well (because if we measure pressures at x_D = 0, then the skin effect also corresponds to this point by Eq. 13).

To demonstrate the points raised above, here we will generate synthetic well-test data using example properties. Then, we will analyze the well-test data by using the conventional techniques[21,22]. The skin estimated from well-test analysis in the examples presented below should match the skin effect at the heel used as input in the analytical model.

Effect of Flux Distribution on Skin Effect.

The main objective of this section is to investigate the effect of skin on horizontal well performance. Unless stated otherwise, we will use the data shown in the Example column of Table 1 for all cases and examples presented here.

First, we will discuss the optimum number of segments required to simulate the flux distribution on an infinite-conductivity horizontal well. As is well known, the flux distribution along an infinite-conductivity horizontal well is U-shaped and symmetric with respect to the mid-point of the well. Because we use a semi-analytical model which discretizes the well, to obtain a good approximation for the flux distribution, a large number of well segments may be required. Figure 7 shows the flux profile during stabilized (pseudoradial) flow period. As can be seen from this figure, after 20 segments, not much improvement is obtained in the flux profile. Therefore, we use 20 segments along the horizontal well in our computations.

In the discussions above, we have found that the skin effect is a function of flux. Because the flux distribution along a horizontal well is a function of time, the skin effect should be a function of time and distance along the wellbore, even when the physical formation damage is uniform. This concept is different from the conventional skin concept for vertical wells.

We have shown that the flux distribution itself is a function of skin also. This has implications on the incorporation of skin effect into horizontal well models. The usual approach is to consider skin pressure drop as an addition to the pressure at the wellbore without skin. Because the flux distribution is different with and without skin, this approach does not work for horizontal wells. To demonstrate this problem, we will compare the pressure responses obtained from the semi-analytical model for three cases:

i) S_{hm} = 0
ii) S_{hm} = 0.5
iii) S_{hm} = 0.5 but the flux distribution corresponds to the S_{hm} = 0 Case (this case matches the conventional modeling of skin for vertical wells).

Fig. 8 shows the differences in pressure responses. Note that Cases ii and iii yield the same responses at early times because the flux distribution is uniform with and without skin. At late times, the flux distributions are different and Case iii does not yield the correct pressure response.

Fig. 9 presents the pressure distribution as a function of distance along the wellbore for the three cases during the early-time radial flow regime. Since the flux is uniform at early times, there is no impact on the pressure response for all cases, which results in a uniform pressure distribution along the wellbore at early time. However, Fig. 10 shows that the pressure profiles along the wellbore are different for the three cases at late times. This result is obtained because of the differences in the flux profiles shown in Figs. 11 and 12.

Examples.

The objective of the examples presented here is to understand the physical meaning of skin estimated from pressure transient analysis by using the standard techniques. We will generate the example data with known input parameters by using the semi-analytical model. Then, we will analyze the data by using the standard straight-line analysis technique and compare the estimates with the original input parameters.

In straight-line analysis, the skin factor is determined from a semi-log plot of early-time radial and late-time pseudoradial flow data. At early times, the following relation is used to estimate the skin factor:[22]

$$S = \frac{1.151kh}{\sqrt{k_y k_z}\,L_h}\left(\frac{\Delta p_{wf}}{m_{er}} - \log t - \log\frac{\sqrt{k_y k_z}}{\phi c_t \mu r_{w,eq}^{\ 2}} + 3.23\right) \tag{15}$$

where m_{er} is the slope of the straight line on the plot of p_{wf} vs. log t at early times given by

$$m_{er} = \frac{162.2q\beta\mu}{\sqrt{k_y k_z}\,L_h} \tag{16}$$

At late times, the skin factor may be computed from the following relation:[22]

$$S = \frac{1.151k}{\sqrt{k_x k_y}}\left(\frac{\Delta p_{wf}}{m_{lr}} - \log t - \log\frac{k}{\phi c_t \mu L_h^{\ 2}} + 1.757\right) - \sqrt{\frac{k}{k_y}}\,(\sigma + F) \tag{17}$$

where m_{lr} is the slope of the straight line of the plot of p_{wf} vs. log t at late times and,

$$\sigma(x_D, y_D) = \left\{\frac{1}{4}\left(x_D - \sqrt{k/k_x}\right)\ln\left[\left(x_D - \sqrt{k/k_x}\right)^2 + y_D^{\ 2}\right] - \left(x_D + \sqrt{k/k_x}\right)\ln\left[\left(x_D + \sqrt{k/k_x}\right)^2 + y_D^{\ 2}\right] + 2y_D\left(arctg\frac{x_D - \sqrt{k/k_x}}{y_D} - arctg\frac{x_D + \sqrt{k/k_x}}{y_D}\right)\right\} \tag{18}$$

which, may be approximated for long horizontal wells by

$$\sigma = \begin{cases} 0 & for \quad uniform\ flux \\ \ln 2 - 1 & for \quad non-uniform\ flux \end{cases} \tag{19}$$

and,

$$F = -\frac{h}{L_h}\sqrt{\frac{k_x}{k_z}}\ln\left\{4\sin\left[\frac{\pi}{2h}\left(2z_w + r_{w,eq}\right)\right]\sin\left(\frac{\pi}{2h}r_{w,eq}\right)\right\} - \varphi \tag{20}$$

In Eq. 20, φ can be neglected for most practical conditions[22] within 1%.

Case 1.

This is the case for an undamaged horizontal well (S_{hm}=0) and is included for comparison.

Case 2.

In this case, the horizontal well has a uniform skin factor of S_{hm} = 0.367 as shown in Fig. 13.

Tables 2 and 3 show the results for Cases 1 and 2 during the early- (ETR), intermediate- (MTR) and late-time regimes (LTR). At early times, the flux distribution is uniform along the wellbore and the skin effect is the same as the skin factor for all horizontal-well segments. The average skin is the same as the skin effect and skin factor. Fig. 15 shows the straight-line analysis during the early-time radial flow regime. Since the flux is uniform and the dimensionless flux is 1.0 during this flow regime, the estimated skin effect is the same as the input value of the skin effect (Eq. 14). In addition, the estimated skin is equal to the mechanical and average skin along the wellbore (0.367).

The results shown in Tables 2 and 3 indicate that the flux varies along the wellbore for both skin cases (S_{hm} = 0 and 0.367) during the middle-time range. Skin effect, however, makes the flux distribution more uniform along the wellbore (Case 2) compared to the no skin case (Case 1). The change of flux along the wellbore also affects the estimation of the skin effect. For example, the average skin is still the same as the mechanical skin but the estimated skin at the heel of the well is higher than the average skin. In most cases, it might be hard to observe a true linear flow regime at intermediate times. One of the main requirements for this flow regime is a long horizontal well. (In our example, we do not have a long enough horizontal well.)

During the late-time pseudoradial flow, the flux distribution along the wellbore for no skin and uniform skin cases is not uniform and the flux ratio changes along the wellbore (it is not 1.0). This change of flux has an impact on the estimation of the skin effect along the wellbore. The skin effect varies along the well and resembles the flux profile. The skin effect at the heel of the well is 0.514, which is higher than the mechanical skin at this location (0.367). The average skin is still the same as the mechanical skin of 0.367. Fig. 16 shows the straight-line analysis of the pseudoradial flow data. The estimated skin (0.512) matches the skin effect at the heel of the well predicted by the model (Table 3). This verifies that what we estimate from the straight-line analysis is the skin effect at the heel of the well, which has the impact of the flux at this location.

Note that in the above examples, we used a uniform mechanical skin (S_{hm}) distribution and the straight-line

analysis technique. If, instead of straight-line analysis, we had used regression analysis, we could have obtained the correct estimate of S_{hm} provided that i) a semi-analytical model similar to the one in this study is used for regression or ii) the skin factor is used as a constant addition to pressure (we have tested this idea by using a commercial software package[20] and estimated the correct mechanical skin). This, however, does not work for non-uniform skin distribution because the regression requires the skin geometry be known a priori. (Theoretically, the skin distribution could be considered as a regression parameter but this would make regression fit practically impossible.)

Case 3.

In this case, the horizontal well has a conical mechanical skin distribution of 0.567 at the heel and 0.167 at the toe. The arithmetic average of skin is 0.367. Fig. 13 shows a sketch of the skin profile and Tables 4 and 5 summarize the model results for Case 3 for the early- (ETR), intermediate- (MTR) and late-time regimes (LTR).

At early times, the flux distribution is uniform along the wellbore and the skin effect is equal to the mechanical skin for all horizontal-well segments. Accordingly, the average skin effect is the same as the average of the mechanical skin (0.367). Fig. 17 shows the straight-line analysis for this skin distribution at early times. As expected, the estimated skin factor is equal to the average skin effect, which is the same as the average mechanical skin.

At intermediate times, the results indicate that the flux varies along the wellbore. (Note that the flux distribution, q_{hs}, is not symmetrical for the conical skin case). The impact of the conical skin distribution along the wellbore causes a conical skin effect also. The average of the skin effect (0.354) is slightly different from the average of the mechanical skin (0.367) and the skin effect at the heel of the well (0.640) is significantly higher than the average skin effect.

During the late-time pseudoradial flow regime, the skin effect at the heel of the well is 0.668, which is higher than the mechanical skin at this location (0.567). The average of the skin effect (0.354) is also slightly different from the average mechanical skin of 0.367. Fig. 18 shows the straight-line analysis for this flow regime. As expected, the straight-line analysis yields the skin effect at the heel of the well (0.663); not the average skin effect along the well (0.354).

Case 4.

The horizontal well in this case has an alternating skin distribution where a damaged segment of $S_{hm} = 1$ is followed by a damaged segment of $S_{hm} = 0.1$ (Fig. 14). A total of 20 equal-length segments are used. The average of the mechanical skin is 0.55.

Tables 6 and 7 show the model results for Case 4 for the early- (ETR), intermediate- (MTR) and late-time regimes (LTR). Because the flux distribution is not uniform at early times, there is only an apparent radial flow regime (and approximate semi-log straight line) and this affects the estimation of the skin effect. To be consistent with the previous cases, we chose 0.19 hour to compute the early-time radial flow results. The average mechanical skin, as an input to the model, is 0.55. The average skin effect is 0.320, which is less than the average mechanical skin. The skin effect at the heel of the well is 0.494, which significantly differs from the mechanical skin of 1.0 at this point.

Fig. 19 shows the straight-line analysis for this skin case at early times. The estimated skin factor is the same as the average skin effect but it is different from the average mechanical skin.

At intermediate times, the average skin effect (0.326) is not the same as the average mechanical skin (0.55) and the skin effect at the heel of the well (0.716) is higher than the average skin effect.

During the late-time pseudoradial flow regime, the flux distribution along the wellbore is not uniform and the flux ratio, q_h/q_{hs}, varies along the wellbore. The skin effect at the heel of the well is 0.747, which is less than the mechanical skin at this location (1.0). The average skin effect (0.326) is not equal to the average mechanical skin (0.55).

Fig. 20 shows the straight-line analysis for pseudoradial flow regime. The skin effect estimated from pseudoradial flow analysis (0.740) is not equal to the average skin effect along the well (0.326) but it is the same as the skin effect at the heel (0.747). It is clear that the skin and flux distributions along the wellbore have affected the estimation of the skin effect.

Case 5.

The horizontal well in this case has a non-uniform mechanical skin distribution as shown in Fig. 14. The arithmetic average of the mechanical skin distribution is 0.55 and the average mechanical skin weighted by the segment length is 0.460. Tables 8 and 9 show the results during the early- (ETR), intermediate- (MTR), and late-time regimes (LTR).

At early times, the arithmetic average skin effect is 0.293, which is lower than the average mechanical skin due to the non-uniform flux distribution and unequal well segments. The average skin effect weighted by length is 0.262. The skin effect at the heel of the well is 0.450 compared to the input mechanical skin of 1.0 at this point.

Fig. 21 shows the straight-line analysis for this skin case during the early-time radial flow regime. The estimated skin factor is the same as the average skin effect (0.293) but it is different from the skin effect at the heel (0.45).

At intermediate times, the impact of non-uniform skin distribution along the wellbore affects the flux distribution and the change of the flux along the wellbore influences the estimation of the skin effect. The arithmetic average of the skin effect (0.323) is not the same as the arithmetic average of the mechanical skin (0.55) and the skin effect at the heel of the well (0.686) is higher than the arithmetic average of the mechanical skin.

At late times, the arithmetic average of the skin effect is 0.324, which is lower than the average mechanical skin due to non-uniform flux distribution and unequal well segments. The average skin effect weighted by the segment length is 0.278. The skin effect at the heel of the well is 0.717 compared to the input mechanical skin of 1.0 at this point.

Fig. 22 shows the straight-line analysis for the late-time pseudoradial flow regime. The estimated skin factor is equal to the skin effect at the heel (0.710) but it is different from the average skin effect and average mechanical skin.

Discussion of Results.
The discussion and the examples presented above indicate the importance of distinguishing between the mechanical skin and the skin effect. The mechanical skin is a measure of the actual formation damage caused by the infiltration of drilling fluids into the formation whereas the skin effect is the contribution of the mechanical skin (formation damage) to the pressure drawdown. This distinction is required for horizontal wells because the skin effect is flux dependent and what is estimated from well-test analysis is the skin effect. This distinction is also useful because the skin effect is the parameter of interest for productivity calculations (as demonstrated in the next section) and the skin factor is the useful parameter for stimulation decisions. It must be emphasized that the above discussion also applies to fractured wells because long horizontal wells behave like fractured wells[22].

For fully penetrating vertical wells, flux distribution is uniform, which makes the skin effect identical to skin factor. For horizontal wells, the flux distribution is non-uniform (except at early times) and time-dependent. This makes the skin effect time dependent until the flux distribution stabilizes at the onset of pseudoradial flow. In addition, because the skin effect is not necessarily equal to the skin factor, the severity of the damage may not be inferred from the well test data. Specifically, the sections of the wellbore with high skin damage (skin factor) have lower flux compared to the sections with lower skin. The combined effect of the skin factor and flux for these sections may yield a smaller skin effect (which should be taken as a measure of the skin pressure drop) that seems to contradict the physical expectations. Therefore, understanding the contribution of the flux distribution on skin effect is extremely useful.

At early times, the flux distribution is uniform for continuously changing skin distributions (such as uniform and conical skin) and practically every segment of the well produces independently of the others. Therefore, the flux has no impact on the skin effect and the skin effect is identical to the skin factor. Furthermore, the arithmetic average skin factor is equal to the arithmetic average skin effect. In cases where the skin damage has jump discontinuities (such as Cases 4 and 5), the flux distribution is not uniform along the entire length. In these cases, the skin factor and skin effect are different locally and the arithmetic average skin factor is different from the arithmetic average skin effect. However, whether the skin distribution is continuos or discontinuous, the skin effect estimated from the pressure-transient analysis of early-time radial flow is the same as the arithmetic average of the skin effect along the wellbore.

At intermediate times, depending on the type of flow regime, different skin effect distributions may exist. If an intermediate-time linear flow period exists, then the flux characteristics will be similar to those for early-time radial flow discussed above and the same conclusions derived there would be valid for intermediate-time linear flow. If the intermediate time flow regime is three-dimensional transitional flow (which is usually the case for most horizontal wells as in the examples considered above), then no simple relationship exists between the skin factor and skin effect locally or as an average. Because there is no specific technique to estimate skin from this flow regime (except regression analysis for uniform skin distribution), we do not discuss the meaning of well-test estimated skin for this case.

At late times, the flux distribution is not uniform but it stabilizes and becomes independent of time at the onset of pseudo-radial flow regime. For continuous skin distributions, higher (arithmetic average) skin factor causes a more uniform flux profile. In general, unless the skin distribution is uniform, the arithmetic average skin factor and arithmetic average skin effect are different during pseudoradial flow. The estimated skin from pressure transient analysis of pseudoradial flow data by using the straight-line technique is the skin effect at the heel of the well. It is not equal to the arithmetic average skin effect or skin factor along the well; nor is it the same as the skin factor at the heel. However, as will be shown in the next chapter, the skin value estimated from well test analysis is the value to be used in productivity equations.

Effect of Skin on Horizontal Well Productivity

In this section, we will demonstrate the importance of using the correct skin values in the evaluation of horizontal well productivity. In the literature,[23] it has been claimed that an average skin effect should be used in horizontal well productivity equations. Our discussions on the skin effect presented in the previous sections (see Eq. 12) show that if the pressures are measured at the heel of the well, then the skin effect at this point should be used for productivity evaluations. Because the skin effect estimated from pseudoradial flow data corresponds to the skin effect at the heel, our proposition has important practical consequences (as shown in Appendix B, calculation of average skin requires a-priori knowledge of the skin zone properties). Appendix B briefly introduces the method suggested by Furui, Zhu and Hill[23] to calculate average skin along a horizontal well. Here we will consider an example to highlight the significance of using the correct skin effect in the calculations.

Productivity Calculation Example.
Here we will present an example to demonstrate the consequences of using the correct skin effect or the average skin as suggested by Furui et al.[23] in the prediction of horizontal well productivities. In this example, we use the semi-analytical model discussed before to generate the synthetic data for a conical skin distribution. For comparison of the results, we use the same general properties for the horizontal well and reservoir as in Ref. 23. The details of the data and the estimation of skin effect for this example are given in Tables 1 and 10.

As shown in Table 10, the analysis of the pressure transient responses during pseudoradial flow period yields a skin effect of 0.908 at the heel of the well. On the other hand, the Furui et. al. model yields the estimates of S_i (from Eq. B-5) and S_{eq} (from Eq. B-4) shown in Table 11. The estimated overall skin factor, $S_{eq,}$ from the Furui et. al. model is 0.447.

It is clear that the skin estimate from well-test analysis and Furui et. al. model are significantly different. (Note that the Furui et. al. model defines the skin factor based on geometrical considerations. The effect of flux is not considered.) We can use the skin estimates by the two methods in the following productivity index equation

presented in Ref. 22 to highlight the consequences of misinterpretation of the skin information:

$$J = \frac{q}{p_i - p_{wf}} = \frac{7.08\times10^{-3} kh}{\beta\mu\left(\ln\frac{2r_e}{L_h} + 1 + \sigma + F + S\right)} \quad (21)$$

where, J is the productivity index, r_e is the reservoir drainage radius, S is the skin effect, and k is the average permeability of the formation, L_h is the horizontal well length, and h is the reservoir thickness. The terms, F and σ are given by Eqs. 20 and 19, respectively.

The results shown in Fig. 23 indicate that the overall skin factor by the method suggested by Furui et al.[23] may significantly overestimate the horizontal well productivity. Figure 24 shows the magnitude of the error.

As a final remark here, we should note that although our results invalidate the use of the overall skin concept for productivity calculations, the mechanical skin formula given by Eq. B-1 of Furui et al.[23] should be useful to generate non-uniform skin distributions for reservoir simulation studies.

Summary and Conclusions

In this study, the effect of near wellbore damage has been modelled for pressure-transient analysis of horizontal wells. It has been emphasized that the conventional definition of skin for vertical wells is not directly applicable to horizontal wells. Also, the impact of misinterpreting the skin effect in horizontal well productivity calculations has been highlighted.

The results of this study indicate that it is useful to distinguish between skin factor and skin effect. Skin factor is a measure of permeability damage whereas skin effect is a measure of the total contribution of formation damage to pressure drawdown. The skin factor estimated from the pressure-transient tests during early-time radial flow is the same as the arithmetic average of the skin effect along the well. The skin estimated from pressure transient tests during pseudoradial flow represents the skin effect at the heel of the well. The correct skin effect to be used in productivity equations is the one determined from pseudoradial flow analysis of pressure-transient data.

Nomenclature

S_{hm} = mechanical skin factor of horizontal well
S = skin effect of horizontal well
x = distance in the x direction, ft
y = distance in the y direction, ft
z = distance in the z direction, ft
z_w = well location in the vertical interval, ft
r = radial distance in the horizontal x-y plane, ft
r_w = wellbore radius, ft
r_{we} = equivalent wellbore radius, ft
r_s = skin zone radius, ft
r_e = reservoir drainage radius, ft
$L = L_h$ = horizontal well length, ft
h = formation thickness, ft
k_h = horizontal permeability of the reservoir, md
$k_v = k_z$ = vertical permeability of the reservoir, md
k = equivalent permeability in x-y-z planes, md
k_r = equivalent permeability in y-z plane, md
k_x = permeability in x-direction, md
k_y = permeability in y-direction, md
k_z = permeability in z-direction, md
k_s = permeability in the skin zone, md
μ = viscosity, cp
ϕ = porosity, fraction
B = formation volume factor, rbbl/stb
c_t = total compressibility, psi^{-1}
t = time, hour
p = pressure, psi
p_s = pressure downstream of the skin zone, psi
p_{wf} = pressure at the heel, psi
p_i = initial reservoir pressure, psi
q = production rate, bbl/d
q_t = total production rate, bbl/d
q_h = flux at the well surface, bbl/d
q_{hs} = flux in case of skin zone, bbl/d
x_D = dimensionless distance in the x direction
y_D = dimensionless distance in the y direction
z_D = dimensionless distance in the z direction
z_{wD} = dimensionless well location in the vertical interval
r_{wD} = dimensionless wellbore radius
L_{hD} = dimensionless horizontal well length
t_D = dimensionless time
p_D = dimensionless pressure
p_{wD} = dimensionless wellbore pressure
q_{hD} = dimensionless flux
q_{hsD} = dimensionless flux in case of skin zone
G = source, or Green, function
N = number of time points
M = number of segments along the horizontal well
J = horizontal well productivity, stb/d/psi

References

1. Van Everdingen, A. F.: "The Skin Effect and its Influence on the Productivity Capacity of the Well," Trans., AIME, (1953) 198.
2. Hurst V.: "Establishment of the Skin Effect and its Impediment to the Flow into a Wellbore," The Petroleum Engineer (Oct. 1953) B-6.
3. Hawkins, M. F. Jr.: "A note on the Skin Effect," Trans. AIME, (1956) 207: 356-357.
4. Kuchuk, F. J., Goode, P. A., Wilkinson, D. J., Thambynayagam, R. K. M.: "Pressure Transient Behavior of Horizontal Wells with and without Gas Cap and Aquifer." paper SPE 17413, presented at the 1988 SPE California Regional Meeting, Long Beach, CA, March 23-25, 1988.
5. Ouyang, L-B.: "Pressure Drawdown Solution for Horizontal Wells in Finite Reservoirs." Well Testing, Vol 2, No 1 (1993).
6. Bob Burton.: "Estimate Formation Damage Effects on Horizontal Wells." Petroleum Engineer International, (August 1995) 29.
7. D.B. Bennion et al., "Fluid Design to Minimize Invasive Damage in Horizontal Wells," paper HWC94-71 presented at the 1994 Canadian SPE/CIM/CANMET International Conference On Recent Advances in Horizontal Well Applications, Calgary, Canada, March 20-23, 1994.
8. G. Chauveteau, L. Nabzar and J-P. Coste.: "Physics and Modeling of Permeability Damage Induced by Particle Deposition," paper SPE 39463 presented at the 1998

International Symposium on Formation Damage Control held in Lafayette, Louisiana, Feb 18-19, 1998.
9. Tim Betty, D. Brant, B. Hebner and R. Hiscock.: "Minimizing Formation Damage in Horizontal Wells: Laboratory and Field Case Studies," paper presented at CIM 1993 Annual Technical Conference in Calgary, May, 1993.
10. M. J. Economides and C.A. Ehlig-Economides.: "Discussion of Formation Damage Effects on Horizontal Well Flow Efficency." JPT (Dec. 1991).
11. J. Yan, G. Jiang and X. Wu.: "Evaluation of Formation Damage Caused by Drilling and Completion Fluids in Horizontal Wells," JCPT (May 1997) V36, No.5
12. D.L. Purvis and D.D. Smith.: "Underbalanced Drilling in the Williston Basion," paper SPE 39924, 1998 SPE Rocky Mountains Regional / Low Permeability Reservoir Symposium., Denver, Colorado, (April 5-8 1998).
13. T.W. Engler, S. Osisanya and D. Tiab.: "Measuring Skin While Drilling," paper SPE 29526 presented at the 1995 Production Operations Symposium, Oklahoma City, April 2-4, 1995.
14. S. B. Toulekima, D.D. Mamora and R.A. Wattanbarger.: "The Effect of Skin Location, Production Interval and Permeability on Performance of Horizontal Wells," Journal of Petroleum Science and Engineering 17 (1997) 63-69.
15. Ozkan, E. and Raghavan, R.: "Estimation of Formation Damage in Horizontal Wells," paper SPE 37511 presented at the 1997 Production Operations Symposium, Oklahoma City, OK, March 9-11, 1997.
16. Raghavan, R.: Well-Test Analysis, Englewood Cliffs, NJ, PTR Prentice Hall (1993).
17. Muskat, M.: Physical Principles of Oil Production, International Human Resources Development Corporation, Boston, Mass. (1981).
18. Gringarten, A. C. and Ramey, H. J., Jr.: "The Use of Source and Green's Functions in Solving Unsteady-Flow Problems in Reservoirs," Soc. Pet. Eng. J. (Oct. 1973).
19. Ozkan, E., Raghavan, R., and Joshi, S. D.: "Horizontal Well Pressure Analysis," SPEFE (Dec. 1989) 567-575.
20. Commercial Well-Testing Software "Saphir", http://www.kappaeng.com/, KAPPA Engineering, France © 1987-2003.
21. Dake, L. P.: Fundamentals of Reservoir Engineering, Elsevier, Amsterdam (1978).
22. Ozkan, E.: Horizontal Wells: Reservoir and Production Aspects, Petroleum Engineering Department, Class Notes, Colorado School of Mines, (Fall 2001).
23. Furui, D. Zhu, and A. D. Hill: "A Rigorous Formation Damage Skin Factor and Reservoir Inflow Model for a Horizontal Well," paper SPE 74698 presented at the 2002 SPE International Symposium and Exhibition, Louisiana, Feb. 20-21, 2002.

Appendix

A. Horizontal Well Pressure-Transient Model

The general pressure transient solution for horizontal wells is usually derived using the method of sources and sinks and green's functions[18]. The dimensionless pressure response for a horizontal well is given by

$$p_D(x_D, r_{wD}, t_D) = \int_o^{t_D} \int_x q_{hD}(x'_D, t'_D) G_D(x_D - x'_D, t_D - t'_D) dx' dt' \quad \text{(A-1)}$$

where, $G_D(x_D, t_D)$ is the instantaneous point-source function given by

$$G_D(x_D, y_D, z_D, t_D) = \frac{\eta}{2L^2 t_D} \sqrt{\frac{k_z}{k}} \exp\left(-\frac{{x_D}^2 + {y_D}^2}{4t_D}\right) \left[1 + 2\sum_{n=1}^{\infty} \exp\left(-\frac{n^2\pi^2 t_D}{{h_D}^2}\right) \cos\left(n\pi \frac{z_D}{h_D}\right) \cos\left(n\pi \frac{z_{wD}}{h_D}\right)\right] \quad \text{(A-2)}$$

The dimensionless flux and pressure are defined by Eqs. 8 and 12, respectively and the other dimensionless variables are defined by

$$t_D = \frac{6.328x10^{-3} k}{\phi c_t \mu (L_h/2)^2} t \quad \text{(A-3)}$$

$$x_D = \frac{x}{L_h/2} \sqrt{\frac{k}{k_x}} \quad \text{(A-4)}$$

$$y_D = \frac{y}{L_h/2} \sqrt{\frac{k}{k_y}} \quad \text{(A-5)}$$

$$z_{wD} = \frac{z_w}{h} = \frac{z_{wD}}{h_D} \quad \text{(A-6)}$$

$$L_D = \frac{L_h}{2h} \sqrt{\frac{k_v}{k}} \quad \text{(A-7)}$$

$$r_{wD} = \frac{r_{we}}{h} = \frac{r_w}{2h} \left[\left(\frac{k}{k_v}\right)^{1/4} + \left(\frac{k_v}{k}\right)^{1/4}\right] \quad \text{(A-8)}$$

To obtain the infinite-conductivity horizontal-well solution, we discretize Eq. A-1 in space and time. We divide the horizontal section of the well into M segments with an equal length of L_s. Thus, Eq. A-1 becomes

$$p_D(x_{Dj}, r_{wD}, t_D) = \int_0^{t_D} \sum_{i=1}^{M} q_{hDi}(t'_D) G_{Di}(x_{Dj}, t_D - t'_D) dt'_D \quad \text{(A-9)}$$

In Eq. A-9, the source function, G_{Di}, is given by

$$G_{Di}(x_{Dj}, t_D) = \frac{\sqrt{\pi}}{4} \left[\left[erf\left(\frac{x_{Dj} - \frac{2i-2}{M}}{2\sqrt{t_D}}\right) - erf\left(\frac{x_{Dj} - \frac{2i}{M}}{2\sqrt{t_D}}\right)\right] \left\{1 + 2\sum_{n=1}^{\infty} \exp\left(-n^2\pi^2 {L_D}^2 t_D\right) \cos\left(n\pi(z_{wD} + r_{wD})\right) \cos\left(n\pi z_{wD}\right)\right\} \frac{1}{\sqrt{t_D}}\right] \quad \text{(A-10)}$$

Equation A-9 can be discretized in time as follow:

$$p_D(x_{Dj}, r_{wD}, t_D) = \sum_{k=1}^{N} \int_{t_{Dk-1}}^{t_{Dk}} \sum_{i=1}^{M} q_{hDi}(t'_D) G_{Di}(x_{Dj}, t_D - t'_D) dt'_D \quad \text{(A-11)}$$

where, N is the number of time points. If we assume that the flux, q_{hDi}, is constant during the time step ($t_{Dk} - t_{Dk-1}$), then Eq. A-11 becomes:

$$p_D(x_{Dj}, r_{wD}, t_D) = \hat{p}_D(x_{Dj}, r_{wD}, t_{DN}) + \sum_{i=1}^{M} q_{hDi}(t_{DN}) \int_0^{t_{DN}-t_{Dk}} G_{Di}(x_{Dj}, t_D - t'_D)\, dt'_D \tag{A-12}$$

where

$$\hat{p}_D(x_{Dj}, r_{wD}, t_{DN}) = \sum_{k=1}^{N-1} \sum_{i=1}^{M} q_{hDi}(t_{Dk}) \left[\int_0^{t_{DN}-t_{Dk-1}} G_{Di}(x_{Dj}, t'_D)\, dt'_D - \int_0^{t_{DN}-t_{Dk}} G_{Di}(x_{Dj}, t'_D)\, dt'_D \right] \tag{A-13}$$

For the infinite-conductivity case, the horizontal well pressure at the wellbore is;

$$p_{wD}(t_{DN}) - \hat{p}_D(x_{Dj}, r_{wD}, t_{DN}) = \sum_{i=1}^{M} q_{hDi}(t_{DN}) \int_0^{t_{DN}-t_{Dk}} G_{Di}(x_{Dj}, t_D - t'_D)\, dt'_D \tag{A-14}$$

Then,

$$p_{wD}(t_{DN}) - \sum_{k=1}^{N-1} \sum_{i=1}^{M} q_{hDi}(t_{Dk}) \left[\int_0^{t_{DN}-t_{Dk-1}} G_{Di}(x_{Dj}, t'_D)\, dt'_D - \int_0^{t_{DN}-t_{Dk}} G_{Di}(x_{Dj}, t'_D)\, dt'_D \right] = \sum_{i=1}^{M} q_{hDi}(t_{DN}) \int_0^{t_{DN}-t_{Dk}} G_{Di}(x_{Dj}, t_D - t'_D)\, dt'_D \tag{A-15}$$

Eq. A-15 should be evaluated at the center of each segment, which results in a set of M equations in M+1 unknowns. Unknowns are $q_{hDi}(t_{DN})$ for i = 1, 2,……,M, and $p_{wD}(t_{DN})$. An additional equation required to solve this set of equations can be obtained by the requirement that the total flux entering the wellbore is the sum of the fluxes entering each segment. Then,

$$\sum_{i=1}^{M} q_{hi}(t) = q_t \tag{A-16}$$

or,

$$\sum_{i=1}^{M} q_{hDi}(t_{DN}) = M \tag{A-17}$$

The computation of the term,

$$\sum_{k=1}^{N-1} \sum_{i=1}^{M} q_{hDi}(t_{Dk}) \left[\int_0^{t_{DN}-t_{Dk-1}} G_{Di}(x_{Dj}, t'_D)\, dt'_D - \int_0^{t_{DN}-t_{Dk}} G_{Di}(x_{Dj}, t'_D)\, dt'_D \right]$$

in Eq. A-15, requires the knowledge of q_{hDi} at old time steps, t_{D1}, t_{D2},…,t_{DN-1}. Thus, Eq. A-15 can be solved in a forward manner in time requiring the inversion of a space matrix only. This solution procedure provides the flux distribution and pressure along the length of an infinite-conductivity horizontal well.

Horizontal Well Model with Skin Effect.

Using Eq. 13, the skin effect can be incorporated into the semi-analytical model given by Eq. A-15 as follows:

$$p_{wD}(t_{DN}) - \sum_{k=1}^{N-1} \sum_{i=1}^{M} q_{hDi}(t_{Dk}) \left[\int_0^{t_{DN}-t_{Dk-1}} G_{Di}(x_{Dj}, t'_D)\, dt'_D - \int_0^{t_{DN}-t_{Dk}} G_{Di}(x_{Dj}, t'_D)\, dt'_D \right] = \sum_{i=1}^{M} q_{hDi}(t_{DN}) \int_0^{t_{DN}-t_{DN-1}} G_{Di}(x_{Dj}, t_D - t'_D)\, dt'_D + q_{hDj}(t_{DN}) S_{hmj} \tag{A-18}$$

Eq. A-18 is evaluated at the center of the j[th] segment (x_{Dj}) where the mechanical skin, S_{hmj}, should be taken into account. The additional equation to solve this system of equations is given by Eq. A-17. Eqs. A-18 and A-17 can be solved in a forward manner in time, which requires a solution of the following matrix.

$$\begin{Bmatrix} 1 & A_{11} & A_{21} & A_{31} & A_{41} & A_{51} & -- & -- & A_{m-1,1} & A_{m1} \\ 1 & A_{12} & A_{22} & A_{32} & A_{42} & A_{52} & -- & -- & A_{m-1,2} & A_{m2} \\ 1 & A_{13} & A_{23} & A_{33} & A_{43} & A_{53} & -- & -- & A_{m-1,3} & A_{m3} \\ 1 & A_{14} & A_{24} & A_{34} & A_{44} & A_{54} & -- & -- & A_{m-1,4} & A_{m4} \\ 1 & A_{15} & A_{25} & A_{35} & A_{45} & A_{55} & -- & -- & A_{m-1,5} & A_{m5} \\ 1 & --. & --. & --. & -- & --. & -- & -- & --- & --- \\ 1 & --. & --. & --. & -- & --. & -- & -- & --- & --- \\ 1 & A_{1,m-1} & A_{2,m-1} & --- & -- & -- & -- & A_{m-1,m-1} & A_{m,m-1} & \\ 1 & A_{1,m} & A_{2,m} & --- & --- & --- & -- & A_{m-1,m} & A_{m,m} & \\ 0 & 1 & 1 & 1 & 1 & 1 & --- & --- & --- & 1 \end{Bmatrix} \begin{Bmatrix} P_{wD} \\ q_{hD1} \\ q_{hD2} \\ q_{hD3} \\ q_{hD4} \\ q_{hD5} \\ .... \\ .... \\ q_{hDM-1} \\ q_{hDM} \end{Bmatrix} = \begin{Bmatrix} B_1 \\ B_2 \\ B_3 \\ B_4 \\ B_5 \\ B_6 \\ .... \\ .... \\ B_M \\ M \end{Bmatrix} \tag{A-19}$$

where the matrix coefficients, A_{ij}, are given by

$$A_{ij} = -\left(\int_0^{t_{DN}-t_{DN-1}} G_{Di}(x_{Dj}, t_D - t'_D)\, dt'_D + S_{hmj} \right) \tag{A-20}$$

The skin is only considered when $i = j$. The right-hand-side vector B_j is obtained by evaluating the following expression at the center of each segment, $x_{Dj:}$

$$B_j = \sum_{k=1}^{N-1} \sum_{i=1}^{M} q_{hDi}(t_{Dk}) \left[\int_0^{t_{DN}-t_{Dk-1}} G_{Di}(x_{Dj}, t'_D)\, dt'_D - \int_0^{t_{DN}-t_{Dk}} G_{Di}(x_{Dj}, t'_D)\, dt'_D \right] \tag{A-21}$$

In Eqs. A-20 and A-21, $G_{Di}(x_{Dj}, t_D)$ is given by

$$G_{Di}(x_{Dj}, t_D) = \frac{\sqrt{\pi}}{4} \left\{ \left[erf\left(\frac{x_{Dj} - \frac{2i-2}{M}}{2\sqrt{t_D}} \right) - erf\left(\frac{x_{Dj} - \frac{2i}{M}}{2\sqrt{t_D}} \right) \right] \left[1 + 2\sum_{n=1}^{\infty} \exp\left(-n^2\pi^2 L_D{}^2 t_D\right) \cos\left(n\pi(z_{wD} + r_{wD})\right) \cos\left(n\pi z_{wD}\right) \right] \frac{1}{\sqrt{t_D}} \right\} \tag{A-22}$$

The dimensionless distance along the horizontal wellbore is given by

$$x_{Dj} = \frac{2j-1}{M} \tag{A-23}$$

The computation of the right-hand-side vector B_j given by Eq. A-21 requires the knowledge of q_{hDi} at the old time steps, which is already known. It must be noted that at very early times, the accuracy of the numerical evaluations is poor. Because at early times flux distribution is uniform and the pressure response is given by the early-time radial flow approximation,[19] we start calculations by using Eq. A-24 and $q_{hD} = 1$ at time $t_D = 10^{-8}$.

$$p_D(t_D, x_D, y_D, z_D) = -\frac{\beta}{8L_D}\sqrt{\frac{k}{k_y}}Ei\left[-\frac{{y_D}^2 + (\tilde{z}_D - \tilde{z}_{wD})^2 / {L_D}^2}{4t_D}\right] \tag{A-24}$$

where

$$\beta = \begin{cases} 2 & if \quad |x_D| < \sqrt{k/k_x} \\ 1 & if \quad |x_D| = \sqrt{k/k_x} \\ 0 & if \quad |x_D| > \sqrt{k/k_x} \end{cases} \tag{A-25}$$

B. Calculation of Average Skin by the Method of Furui et. al.

The skin factor model proposed by Furui, Zhu, Hill[23] considers the effect of damage in the y-z plane perpendicular to the well axis. Using Hawkins' formula,[3] Furui et. al.[23] developed the following thick-skin formula for horizontal well skin factor in an anisotropic formation:

$$s(x) = \left[\frac{k}{k_d(x)} - 1\right]\ln\left[\frac{1}{I_{ani}+1}\left(\frac{r_{dH}(x)}{r_w} + \sqrt{\left(\frac{r_{dH}(x)}{r_w}\right)^2 + {I_{ani}}^2 + 1}\right)\right] \tag{B-1}$$

where

$$I_{ani} = \sqrt{\frac{k_H}{k_V}} \tag{B-2}$$

In Eq. B-1, r_{dH} is the half-length of the horizontal axis of the damage ellipse, r_w is the wellbore radius, k_d is the permeability in the damaged zone, and k is the undamaged permeability. Assuming radial flow concentric with the horizontal wellbore, they obtained the following relationship between the equivalent (overall) skin and local skin for isotropic reservoirs:[23]

$$S_{eq} = \frac{L_h}{\int_o^{L_h}\left\{\ln\left[\frac{h}{2r_w}\right] + s(x)\right\}^{-1} dx} - \ln\left[\frac{h}{2r_w}\right] \tag{B-3}$$

Rewriting Eq. B-3 in the form of a Riemann sum over 0 to L gives

$$S_{eq} = \frac{L_h}{\sum_{i=1}^{N}\left\{\frac{\Delta L_i}{\ln[h/(2r_w)] + s_i}\right\}} - \ln\left[\frac{h}{2r_w}\right] \tag{B-4}$$

where N is the total number of segments, and

$$S_i = \left[\frac{k}{k_{d,i}} - 1\right]\ln\left(\frac{r_{d,i}}{r_w}\right) \tag{B-5}$$

For anisotropic reservoirs, the relationship between the equivalent (overall) skin and local skin is given by[23]

$$S_{eq} = \frac{L_h}{\int_o^{L_h}\left\{\left[\frac{I_{ani}h}{r_w(I_{ani}+1)}\right] + s(x)\right\}^{-1} dx} - \ln\left[\frac{I_{ani}h}{r_w(I_{ani}+1)}\right] \tag{B-6}$$

Rewriting Eq. B-6 in the form of a Riemann sum over 0 to L gives

$$S_{eq} = \frac{L_h}{\sum_{i=1}^{N}\frac{\Delta L_i}{\left[\frac{I_{ani}h}{r_w(I_{ani}+1)}\right] + S_i}} - \ln\left[\frac{I_{ani}h}{r_w(I_{ani}+1)}\right] \tag{B-7}$$

where N is the total number of segments, and S_i is given by Eq. B-5. Note that the relations given in Eqs. B-3 and B-6 require that the skin zone properties be known.

Table 1 – Horizontal well and reservoir data

	Comparison Case 1 - data	Comparison Case 2- data	Skin Cases data	Productivity Example data
h, ft	50	84	110	100
μ_o, cp	1.2	1.2	1.5	1.2
β_o, rb/stb	1.12	1.12	1.5	1.12
r_w, in	4.25	4.25	5.5	4.25
q, stb/d	1000	5000	2000	2000
ϕ, fraction	0.2	0.24	0.1	0.1
c_t, psi^{-1}	$4x10^{-5}$	$5.5x10^{-5}$	$3x10^{-5}$	$3x10^{-5}$
L_h, ft	2000	2626	1500	2000
z_w, ft	25	52	55	50
k_x, md	50	100	50	50
k_y, md	50	150	100	50
k_z, md	50	50	25	50
p_r, psi	4000	4000	4000	4000
S_{hm} - case 1	0.0	0.0	-	-
S_{hm} - case 2	0.5	0.75	-	-

Table 2 – Flux ratio for Case 2 at different times

		ETR	MTR	LTR
Seg. No.	x (ft)	q_h/q_{hs}	q_h/q_{hs}	q_h/q_{hs}
1	37.5	1.000	1.175	1.191
2	112.5	1.000	1.058	1.067
3	187.5	1.000	1.010	1.014
4	262.5	1.000	0.981	0.981
5	337.5	1.000	0.963	0.959
6	412.5	1.000	0.952	0.944
7	487.5	1.000	0.944	0.934
8	562.5	1.000	0.940	0.927
9	637.5	1.000	0.937	0.923
10	712.5	1.000	0.936	0.921
11	787.5	1.000	0.936	0.921
12	862.5	1.000	0.937	0.923
13	937.5	1.000	0.940	0.927
14	1012.5	1.000	0.944	0.934
15	1087.5	1.000	0.952	0.944
16	1162.5	1.000	0.963	0.959
17	1237.5	1.000	0.981	0.981
18	1312.5	1.000	1.010	1.014
19	1387.5	1.000	1.058	1.067
20	1462.5	1.000	1.175	1.191

Table 3 – Skin effect for Case 2 at different times

	ETR		MTR		LTR	
Seg. No.	$S_{hm}(x)$	S(x,t)	$S_{hm}(x)$	S(x,t)	$S_{hm}(x)$	S(x,t)
1	0.367	0.367	0.367	0.495	0.367	0.514
2	0.367	0.367	0.367	0.428	0.367	0.440
3	0.367	0.367	0.367	0.392	0.367	0.399
4	0.367	0.367	0.367	0.368	0.367	0.370
5	0.367	0.367	0.367	0.352	0.367	0.350
6	0.367	0.367	0.367	0.339	0.367	0.335
7	0.367	0.367	0.367	0.331	0.367	0.324
8	0.367	0.367	0.367	0.325	0.367	0.317
9	0.367	0.367	0.367	0.321	0.367	0.312
10	0.367	0.367	0.367	0.319	0.367	0.310
11	0.367	0.367	0.367	0.319	0.367	0.310
12	0.367	0.367	0.367	0.321	0.367	0.312
13	0.367	0.367	0.367	0.325	0.367	0.317
14	0.367	0.367	0.367	0.331	0.367	0.324
15	0.367	0.367	0.367	0.339	0.367	0.335
16	0.367	0.367	0.367	0.352	0.367	0.350
17	0.367	0.367	0.367	0.368	0.367	0.370
18	0.367	0.367	0.367	0.392	0.367	0.399
19	0.367	0.367	0.367	0.428	0.367	0.440
20	0.367	0.367	0.367	0.495	0.367	0.514
Avg. (Arithmetic)	0.367	0.367	0.367	0.367	0.367	0.367
Avg. (Weighted by Length)	0.367	0.367	0.367	0.367	0.367	0.367

Table 4 – Flux ratio for Case 3 at different times

		ETR	MTR	LTR
Seg. No.	x (ft)	q_h/q_{hs}	q_h/q_{hs}	q_h/q_{hs}
1	37.5	1.000	1.403	1.415
2	112.5	1.000	1.214	1.218
3	187.5	1.000	1.130	1.128
4	262.5	1.000	1.076	1.070
5	337.5	1.000	1.040	1.029
6	412.5	1.000	1.013	1.000
7	487.5	1.000	0.993	0.977
8	562.5	1.000	0.976	0.960
9	637.5	1.000	0.963	0.947
10	712.5	1.000	0.952	0.936
11	787.5	1.000	0.942	0.928
12	862.5	1.000	0.933	0.921
13	937.5	1.000	0.926	0.916
14	1012.5	1.000	0.919	0.912
15	1087.5	1.000	0.914	0.910
16	1162.5	1.000	0.910	0.910
17	1237.5	1.000	0.908	0.913
18	1312.5	1.000	0.910	0.919
19	1387.5	1.000	0.918	0.932
20	1462.5	1.000	0.956	0.975

Table 5 – Skin effect for Case 3 at different times

	ETR		MTR		LTR	
Seg. No.	$S_{hm}(x)$	S(x,t)	$S_{hm}(x)$	S(x,t)	$S_{hm}(x)$	S(x,t)
1	0.567	0.567	0.567	0.640	0.567	0.668
2	0.546	0.546	0.546	0.555	0.546	0.573
3	0.525	0.525	0.525	0.501	0.525	0.512
4	0.504	0.504	0.504	0.461	0.504	0.466
5	0.483	0.483	0.483	0.428	0.483	0.429
6	0.462	0.462	0.462	0.401	0.462	0.398
7	0.440	0.440	0.440	0.378	0.440	0.372
8	0.419	0.419	0.419	0.357	0.419	0.349
9	0.398	0.398	0.398	0.339	0.398	0.330
10	0.377	0.377	0.377	0.322	0.377	0.313
11	0.356	0.356	0.356	0.307	0.356	0.298
12	0.335	0.335	0.335	0.294	0.335	0.285
13	0.314	0.314	0.314	0.282	0.314	0.274
14	0.293	0.293	0.293	0.271	0.293	0.265
15	0.272	0.272	0.272	0.262	0.272	0.257
16	0.251	0.251	0.251	0.254	0.251	0.252
17	0.229	0.229	0.229	0.249	0.229	0.249
18	0.208	0.208	0.208	0.247	0.208	0.250
19	0.187	0.187	0.187	0.251	0.187	0.257
20	0.167	0.167	0.167	0.276	0.167	0.286
Avg. (Arithmetic)	0.367	0.367	0.367	0.354	0.367	0.354
Avg. (Weighted by Length)	0.367	0.367	0.367	0.354	0.367	0.354

Table 6 – Flux ratio for Case 4 at different times

		ETR	MTR	LTR
Seg. No.	x (ft)	q_h/q_{hs}	q_h/q_{hs}	q_h/q_{hs}
1	37.5	2.051	2.209	2.232
2	112.5	0.661	0.680	0.684
3	187.5	2.044	1.979	1.981
4	262.5	0.661	0.644	0.642
5	337.5	2.044	1.913	1.900
6	412.5	0.661	0.630	0.624
7	487.5	2.044	1.888	1.865
8	562.5	0.661	0.626	0.617
9	637.5	2.044	1.881	1.853
10	712.5	0.661	0.625	0.616
11	787.5	2.044	1.884	1.856
12	862.5	0.661	0.628	0.619
13	937.5	2.044	1.897	1.875
14	1012.5	0.661	0.634	0.629
15	1087.5	2.044	1.927	1.915
16	1162.5	0.661	0.649	0.648
17	1237.5	2.044	1.993	1.997
18	1312.5	0.661	0.683	0.687
19	1387.5	2.044	2.162	2.187
20	1462.5	0.668	0.809	0.822

Table 7 – Skin effect for Case 4 at different times

	ETR		MTR		LTR	
Seg. No.	$S_{hm}(x)$	S(x,t)	$S_{hm}(x)$	S(x,t)	$S_{hm}(x)$	S(x,t)
1	1.000	0.494	1.000	0.716	1.000	0.747
2	0.100	0.151	0.100	0.181	0.100	0.187
3	1.000	0.489	1.000	0.545	1.000	0.556
4	0.100	0.151	0.100	0.153	0.100	0.154
5	1.000	0.489	1.000	0.482	1.000	0.481
6	0.100	0.151	0.100	0.140	0.100	0.138
7	1.000	0.489	1.000	0.451	1.000	0.442
8	0.100	0.151	0.100	0.133	0.100	0.130
9	1.000	0.489	1.000	0.436	1.000	0.423
10	0.100	0.151	0.100	0.130	0.100	0.126
11	1.000	0.489	1.000	0.432	1.000	0.418
12	0.100	0.151	0.100	0.130	0.100	0.127
13	1.000	0.489	1.000	0.438	1.000	0.427
14	0.100	0.151	0.100	0.134	0.100	0.131
15	1.000	0.489	1.000	0.457	1.000	0.450
16	0.100	0.151	0.100	0.142	0.100	0.141
17	1.000	0.489	1.000	0.494	1.000	0.496
18	0.100	0.151	0.100	0.158	0.100	0.160
19	1.000	0.489	1.000	0.571	1.000	0.585
20	0.100	0.152	0.100	0.196	0.100	0.203
Avg. (Arithmetic)	0.550	0.320	0.550	0.326	0.550	0.326
Avg. (Weighted by Length)	0.550	0.320	0.550	0.326	0.550	0.326

Table 8 – Flux ratio for Case 5 at different times

		ETR	MTR	LTR
Seg. No.	x (ft)	q_h/q_{hs}	q_h/q_{hs}	q_h/q_{hs}
1	37.5	2.325	2.308	2.325
2	187.5	0.719	0.718	0.719
3	412.5	1.846	1.859	1.846
4	712.5	0.710	0.720	0.710
5	787.5	2.042	2.069	2.042
6	937.5	0.685	0.692	0.685
7	1162.5	1.902	1.907	1.902
8	1462.5	0.850	0.839	0.850

Table 9 – Skin effect for Case 5 at different times

	ETR		MTR		LTR	
Seg. No.	$S_{hm}(x)$	S(x,t)	$S_{hm}(x)$	S(x,t)	$S_{hm}(x)$	S(x,t)
1	1.000	0.450	1.000	0.686	1.000	0.717
2	0.100	0.137	0.100	0.161	0.100	0.165
3	1.000	0.449	1.000	0.500	1.000	0.499
4	0.100	0.137	0.100	0.115	0.100	0.112
5	1.000	0.446	1.000	0.393	1.000	0.380
6	0.100	0.137	0.100	0.119	0.100	0.116
7	1.000	0.449	1.000	0.464	1.000	0.456
8	0.100	0.137	0.100	0.145	0.100	0.148
Avg. (Arithmetic)	0.550	0.293	0.550	0.323	0.550	0.324
Avg. (Weighted by Length)	0.460	0.262	0.460	0.279	0.460	0.278

Table 10 – Model results for productivity example.

Seg. No.	x ft	$q_{hs}(x,t)$	$q_h(x,t)$	q_h/q_{hs}	$S_{hm}(x)$	S(x,t)
1	100	90.335	202.672	2.244	1.005	0.908
2	200	85.289	134.409	1.576	0.924	0.788
3	300	82.451	108.673	1.318	0.848	0.699
4	400	80.724	94.624	1.172	0.776	0.627
5	500	79.548	85.917	1.080	0.710	0.564
6	600	78.991	80.172	1.015	0.647	0.511
7	700	78.868	76.295	0.967	0.588	0.464
8	800	79.121	73.719	0.932	0.533	0.422
9	900	79.841	72.137	0.904	0.481	0.384
10	1000	80.916	71.382	0.882	0.433	0.350
11	1100	82.495	71.382	0.865	0.388	0.320
12	1200	84.808	72.137	0.851	0.345	0.293
13	1300	87.862	73.719	0.839	0.305	0.268
14	1400	91.873	76.295	0.830	0.268	0.247
15	1500	97.169	80.172	0.825	0.234	0.227
16	1600	104.867	85.917	0.819	0.201	0.211
17	1700	115.717	94.624	0.818	0.171	0.198
18	1800	132.071	108.673	0.823	0.144	0.190
19	1900	160.824	134.409	0.836	0.118	0.190
20	2000	226.230	202.672	0.896	0.094	0.214
			Average (Arithmetic)		0.461	0.404

Table 11 – The results of skin model suggested by Ref. 23

Segment No.	X, ft	Kdi, md	rdi, ft	Si
1	100	25.4	1.000	1.005
2	200	26.1	0.974	0.924
3	300	26.9	0.947	0.848
4	400	27.6	0.921	0.776
5	500	28.3	0.895	0.710
6	600	29.1	0.869	0.647
7	700	29.8	0.842	0.588
8	800	30.5	0.816	0.533
9	900	31.2	0.790	0.481
10	1000	32.0	0.763	0.433
11	1100	32.7	0.737	0.388
12	1200	33.4	0.711	0.345
13	1300	34.2	0.684	0.305
14	1400	34.9	0.658	0.268
15	1500	35.6	0.632	0.234
16	1600	36.4	0.606	0.201
17	1700	37.1	0.579	0.171
18	1800	37.8	0.553	0.144
19	1900	38.5	0.527	0.118
20	2000	39.3	0.500	0.094
			Average	**0.461**
			Seq	**0.447**

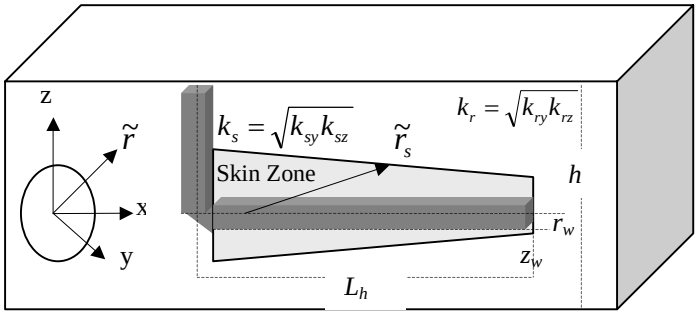

Fig. 1- Horizontal well model (Skin geometry)

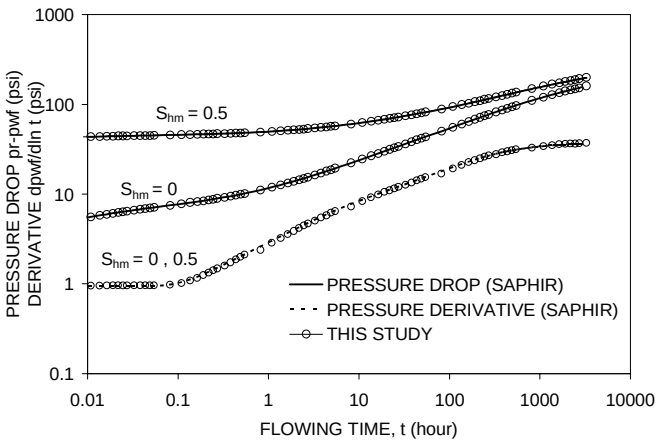

Fig. 2- Pressure transient responses for Comparison Case 1

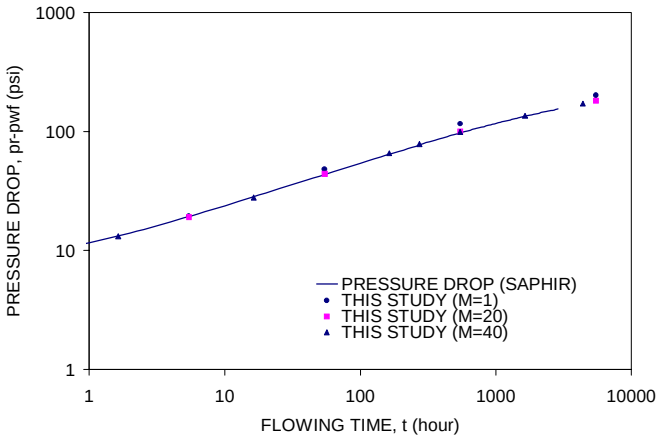

Fig. 3- Number of segments and pressure responses of infinite-conductivity well

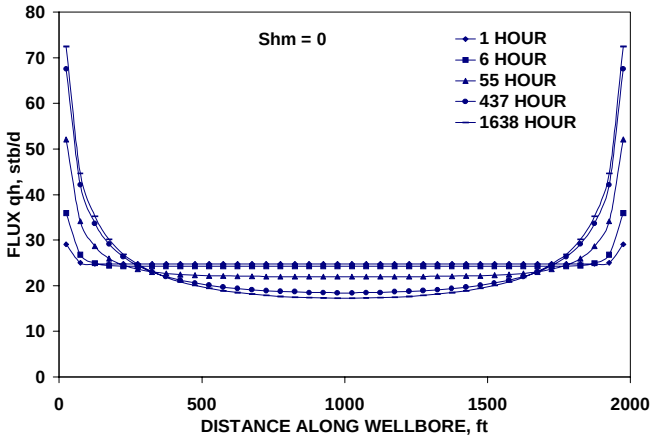

Fig. 4- Flux distribution as function of time for no skin case

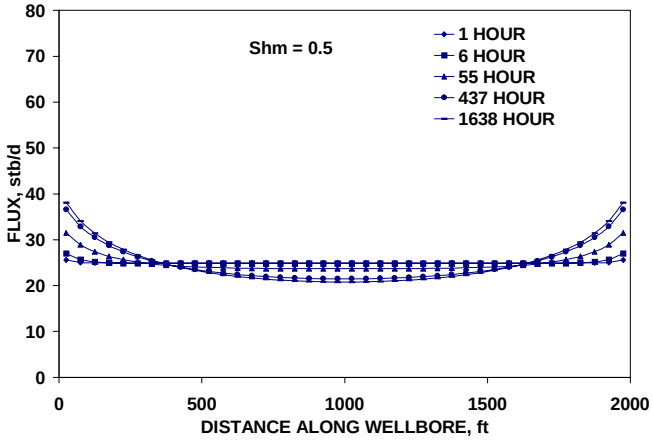

Fig. 5- Flux distribution as function of time for uniform skin of 0.5

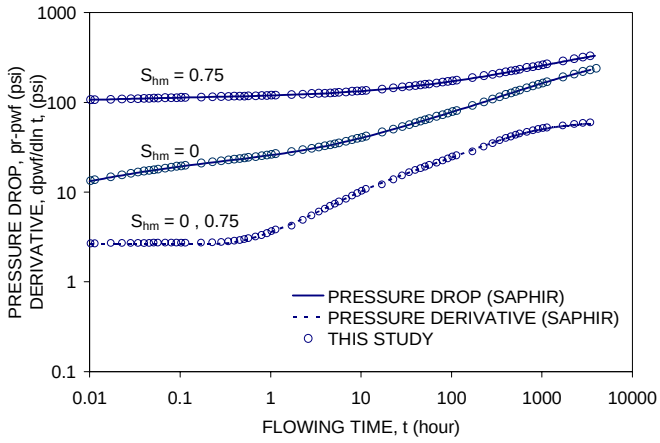

Fig. 6- Pressure transient responses for Comparison Case 2

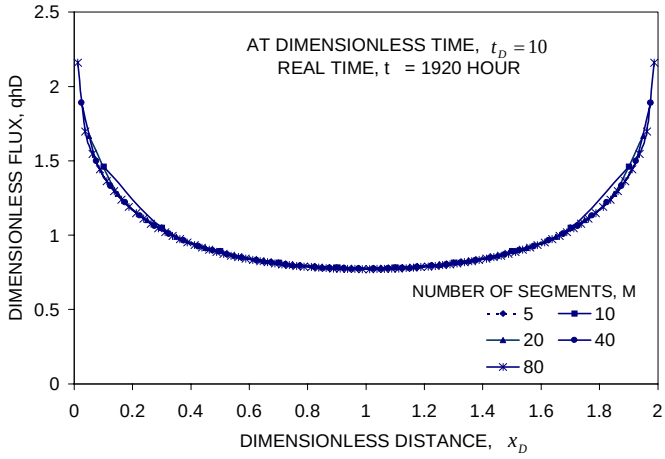

Fig. 7- Sensitivity of number of segments on the flux distribution at the late time.

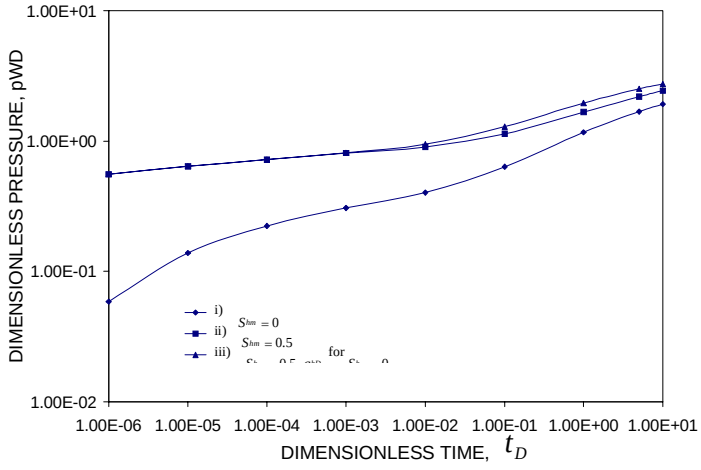

Fig. 8- Effect of skin on horizontal well pressure response

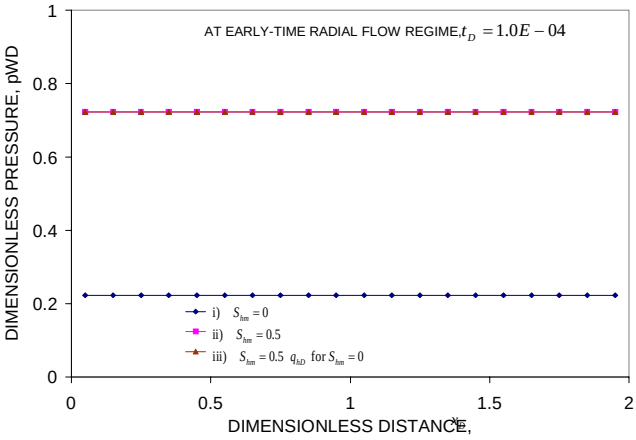

Fig. 9- Effect of skin on horizontal well pressure response at early-time

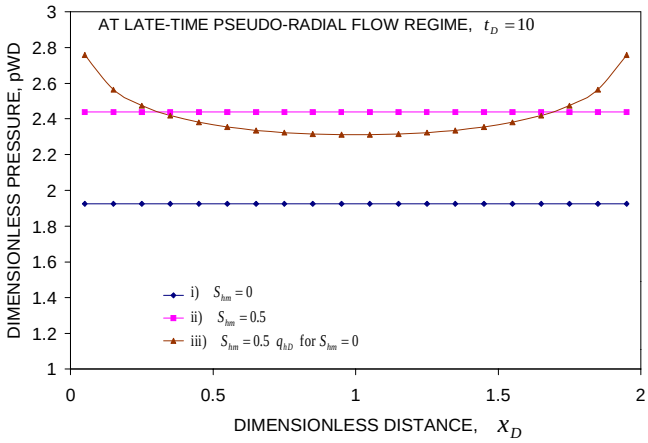

Fig. 10- Effect of skin on horizontal well pressure response at late-time

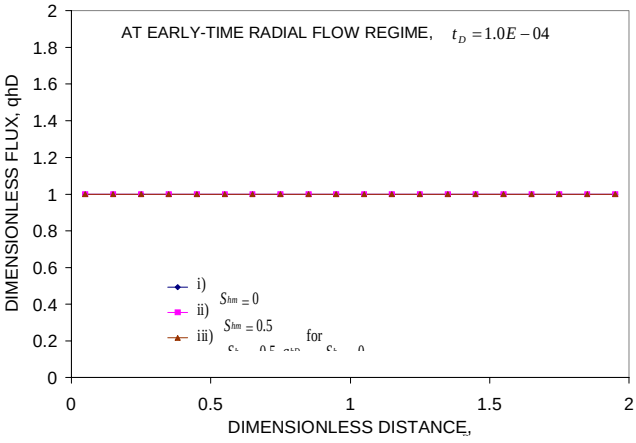

Fig. 11- Early-time radial flow flux distribution along the horizontal wellbore

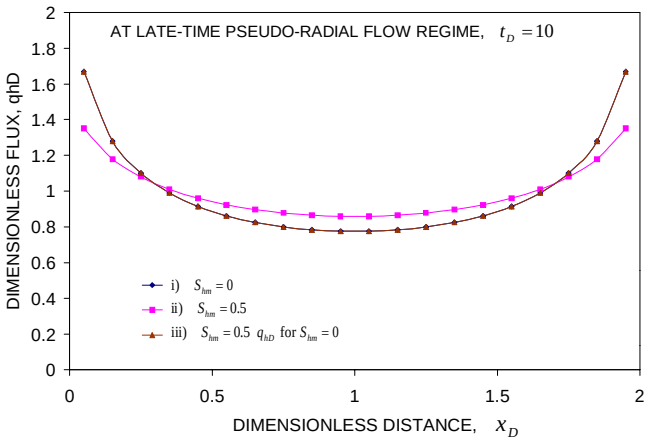

Fig. 12- Late-time pseudoradial flow flux distribution along the wellbore

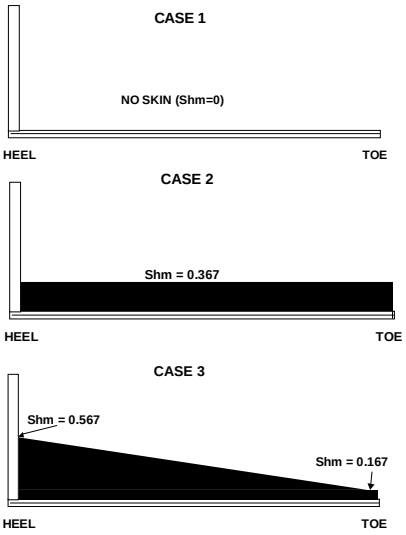

Fig. 13- Skin geometry for Cases 1, 2 and 3

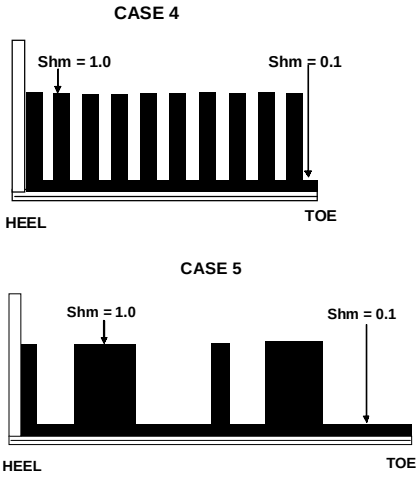

Fig. 14- Skin geometry for Cases 4 and 5

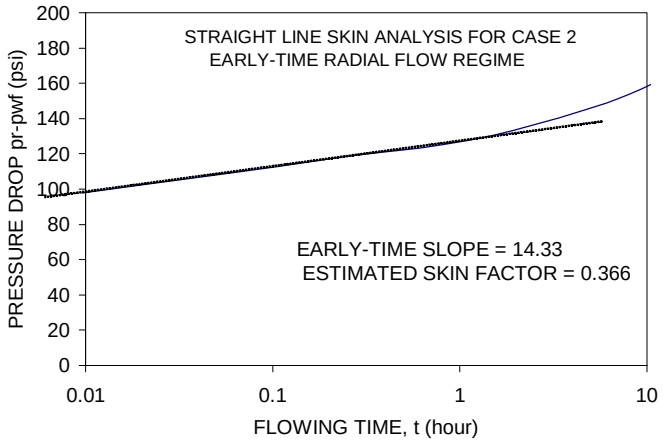

Fig. 15- Early-time straight-line analysis for Case 2

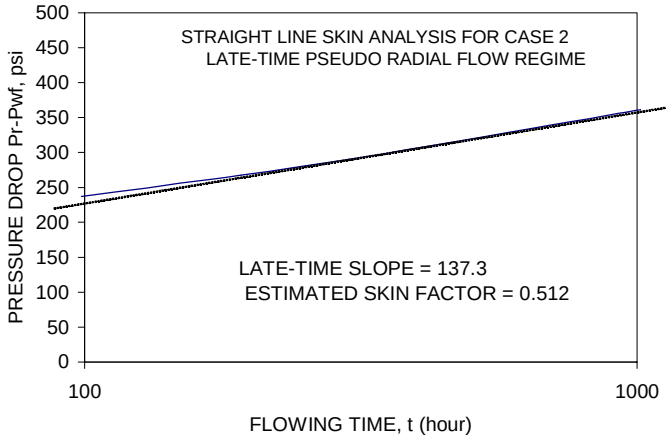

Fig. 16- Late-time straight-line analysis for Case 2

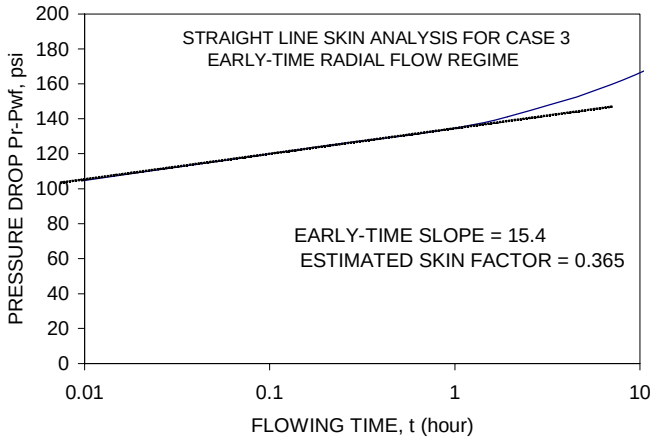

Fig. 17- Early-time straight-line analysis for Case 3

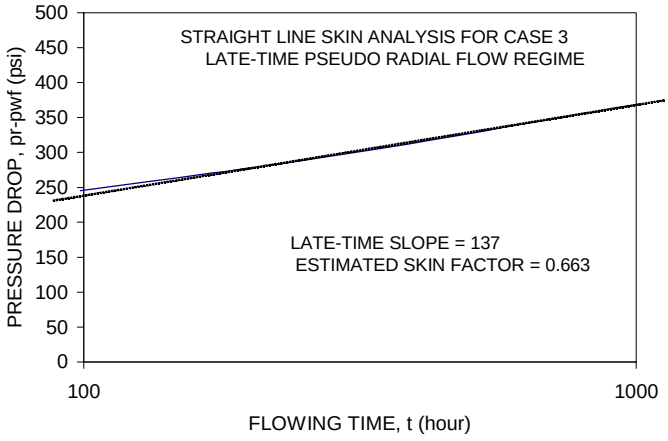

Fig. 18- Late-time straight-line analysis for Case 3

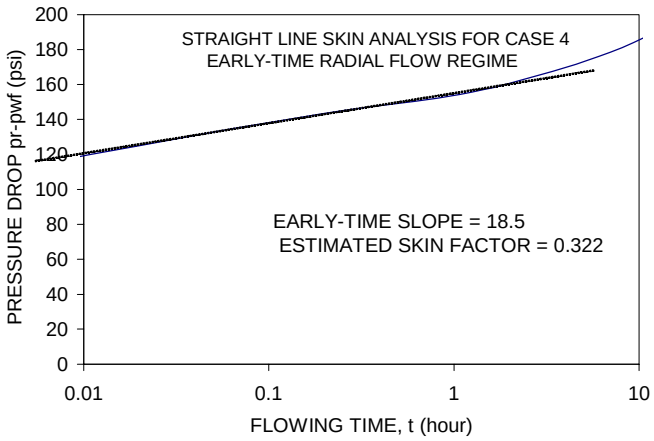

Fig. 19- Early-time straight-line analysis for Case 4

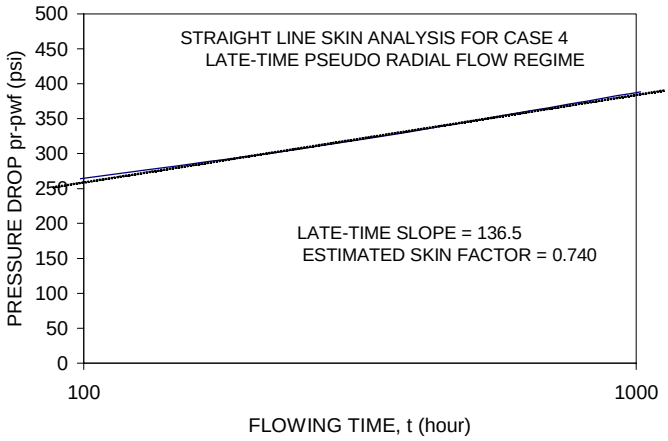

Fig. 20- Late-time straight-line analysis for Case 4

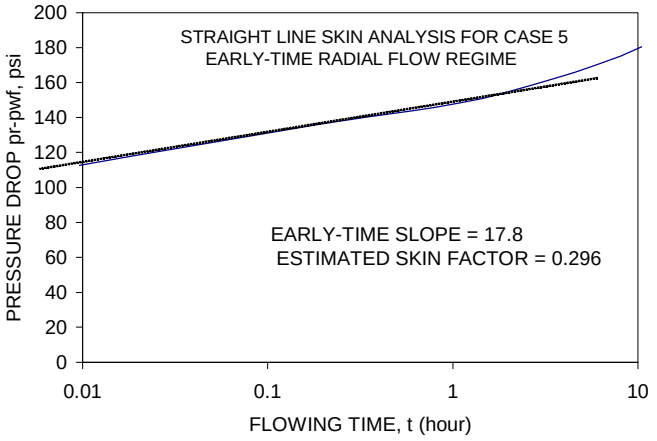

Fig. 21- Early-time straight-line analysis for Case 5

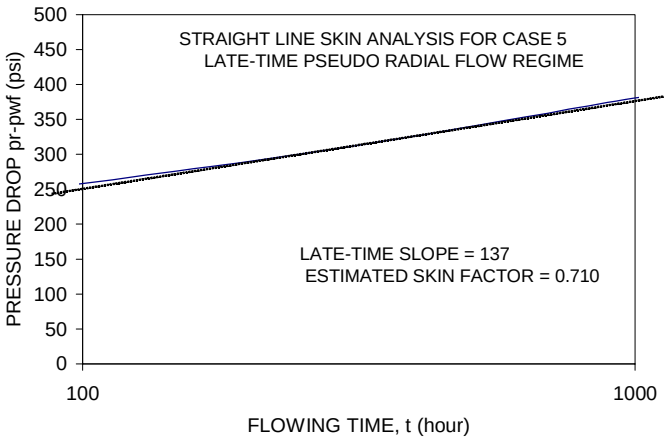

Fig. 22- Late-time straight-line analysis for Case 5

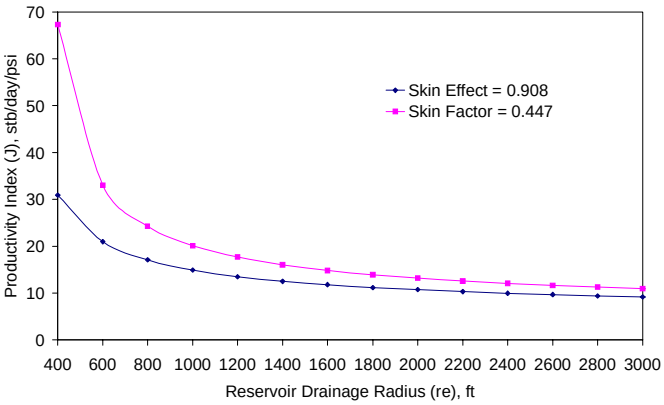

Fig. 23- Effect of skin on horizontal well productivity index

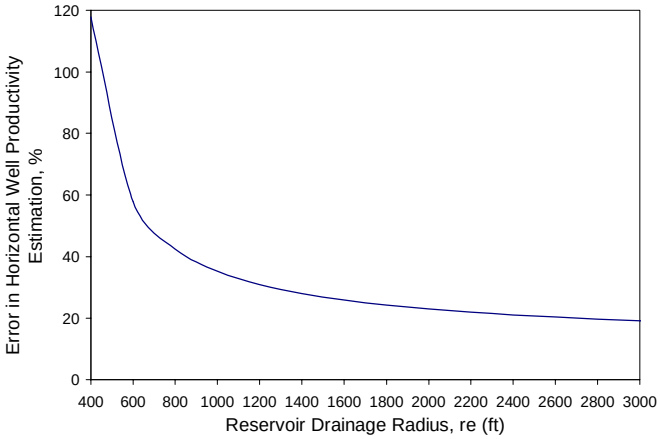

Fig. 24- Error in estimating the productivity index using the overall skin concept